Published in final edited form as:

Nat Neurosci. 2009 May ; 12(5): 577–584. doi:10.1038/nn.2307.

Hyperpolarization-activated cation channels inhibit EPSPs by interactions with M-type K^+ channels

Meena S. George[1], **L.F. Abbott**[1,2], and **Steven A. Siegelbaum**[1,3,4]

[1]Department of Neuroscience Columbia University, 1051 Riverside Drive, New York, NY 10032, USA

[2]Department of Physiology and Cellular Biophysics Columbia University, 1051 Riverside Drive, New York, NY 10032, USA

[3]Department of Pharmacology Columbia University, 1051 Riverside Drive, New York, NY 10032, USA

[4]Howard Hughes Medical Institute Columbia University, 1051 Riverside Drive, New York, NY 10032, USA

Abstract

The processing of synaptic potentials by neuronal dendrites depends on both their passive cable properties and active voltage-gated channels, which can generate complex effects due to their nonlinear properties. In this study, we characterized the actions of the hyperpolarization-activated cation current (I_h) on dendritic processing of subthreshold excitatory postsynaptic potentials (EPSPs) in mouse CA1 hippocampal neurons. Although I_h generates an excitatory inward current that exerted a direct depolarizing effect on the peak voltage of weak EPSPs, it produced a paradoxical hyperpolarizing effect on the peak voltage of stronger but still subthreshold EPSPs. Using a combined modeling and experimental approach, we found that the inhibitory action of I_h is caused by its interaction with the delayed rectifier M-type K^+ current. In this manner, I_h can enhance spike firing in response to an EPSP when spike threshold is low but inhibit firing when spike threshold is high.

Introduction

Neurons actively process and integrate synaptic potentials through the actions of a wide array of voltage-gated ion channels that are often differentially expressed throughout a neuron's dendritic tree1. In some instances, the effects of voltage-gated channels on dendritic processing are relatively straightforward and well understood. For example, dendritic voltage-gated sodium and calcium channels can amplify synaptic potentials2

Correspondence: sas8@columbia.edu.

AUTHOR CONTRIBUTIONS

M.S.G. performed all experiments, wrote the computer programs, performed the analysis, and wrote the initial draft of the manuscript. L.F.A. and S.A.S. participated in the design of the experiments and modeling studies and helped in the preparation of the final manuscript.

through the generation of local or propagated dendritic action potentials3, 4. In contrast, dendritic voltage-gated or calcium-activated K^+ channels can reduce EPSP amplitude and dampen dendritic excitability5-7. However, in other cases, nonlinear interactions between dendritic voltage-gated channels give rise to complex effects that are less easily understood. In this study we focus on the paradoxical effects of the hyperpolarization-activated HCN cation channels on the processing of EPSPs in the apical dendrites of CA1 pyramidal neurons, where these channels are expressed in a gradient of increasing density with increasing distance from the soma8-11.

Unlike most voltage-gated channels, HCN channels activate with hyperpolarization and deactivate with depolarization. Their mixed permeability to K^+ and Na^+ ions results in a reversal potential (E_h) of approximately −30 mV, causing these channels to generate an excitatory inward current (I_h) at subthreshold potentials. These biophysical properties underlie the role of I_h as a pacemaker current in cardiac myocytes and thalamocortical relay neurons, where activation of I_h following action potential repolarization generates a depolarizing current that drives spontaneous, rhythmic firing12, 13. In neurons that are not spontaneously active, I_h contributes a 5–10 mV depolarizing influence on the resting membrane potential and increases the resting membrane conductance (that is, it lowers the input resistance), thereby regulating the spatial and temporal integration of synaptic inputs10, 14-16.

Despite the fact that I_h provides a depolarizing current at subthreshold potentials, several studies indicate that it has a paradoxical inhibitory effect on the ability of an EPSP to trigger an action potential. Thus, enhancement of I_h – by the anticonvulsant lamotrigine17, application of dopamine18, or induction of long-term potentiation19, 20 – decreases excitability and spike firing. Conversely, downregulation of I_h – through genetic deletion of HCN121, pharmacological blockade using cesium15, 22 or the organic antagonist ZD728815, 16, or following induction of long-term depression23 or seizures24 – increases EPSP amplitude, temporal summation, and spike firing.

The inhibitory effects of I_h, by which we mean the inhibition seen when I_h is enhanced, have generally been attributed to its action to increase the resting membrane conductance. This so-called ‘shunting effect’ on the excitatory postsynaptic current decreases the amplitude of an EPSP10, 22, where EPSP amplitude (ΔV_{EPSP}) is defined as the difference between the peak voltage of an EPSP (V_{peak}) and the resting potential. However, the impact of an EPSP depends not on its amplitude but on the voltage reached at its peak, which determines whether an EPSP is suprathreshold25. Importantly, I_h exerts two opposing influences on V_{peak}: its shunting effect decreases EPSP peak voltage whereas its direct depolarizing effect increases V_{peak} (see Fig. 1a).

In this study, we first show in a simple computational model that, in the absence of other voltage-gated conductances, I_h should be always excitatory for EPSPs negative to the I_h reversal potential—that is, the depolarizing action of I_h on V_{peak} is always greater than its shunting effect. This implies that any inhibitory effect of I_h on V_{peak} must be caused by its interactions with other voltage-gated conductances.

One such interaction results in an inhibitory effect of I_h on the duration of Ca^{2+} action potentials in the distal dendrites of CA1 pyramidal neurons26. In this instance, the depolarizing effect of I_h on the resting membrane increases the resting inactivation of N- and T-type voltage-gated Ca^{2+} channels, thus inhibiting the Ca^{2+} spikes. In principle, this effect of I_h on resting potential and resting inactivation could also explain how I_h suppresses the firing of Na^+ action potentials. However, it remains unclear whether I_h can exert an inhibitory effect on V_{peak} for subthreshold EPSPs.

Here, we found that I_h, through interactions with voltage-gated K^+ channels, could indeed produce an inhibitory effect on peak voltage of subthreshold EPSPs. Interestingly, the influence of I_h on V_{peak} depended on synaptic strength. Thus, whereas I_h shifted V_{peak} to more positive potentials for weak EPSPs, I_h inhibited V_{peak} for stronger, but still subthreshold, EPSPs. In other words, the effects of I_h on V_{peak} crossed over from depolarizing to hyperpolarizing as a function of increasing synaptic strength, with the "crossover" potential occurring below both the reversal potential for I_h and the action potential threshold. This indicated that the net effect of I_h is essentially inhibitory as it made it more difficult for an EPSP to reach threshold. Both our computational and experimental results demonstrated that the inhibitory effect of I_h was caused by its action to depolarize the resting membrane, which enhanced the resting activation of the delayed-rectifier M-type K^+ channels. Because the M-channels are under neuromodulatory control27, the influence of I_h on dendritic integration may switch from inhibitory to excitatory depending on the state of M-channel regulation. Such modulation may have important implications for regulation of long-term synaptic plasticity that contributes to learning and memory21, 28, and for the treatment of epileptic disorders in which both I_h and M-channels may play a role29-32.

RESULTS

Dual influence of I_h on EPSPs in CA1 pyramidal neurons

We first examined the influence of I_h on neuronal activity in mouse hippocampal CA1 pyramidal neurons by performing whole-cell current-clamp recordings of both resting membrane properties and somatic EPSPs evoked by stimulation of the Schaffer collateral pathway (Fig. 1b). In response to hyperpolarizing current steps injected in the CA1 neuron soma, the membrane voltage exhibited a depolarizing sag that is characteristic of I_h activation (Fig. 1c). We then applied focal synaptic stimulation of increasing strength to elicit EPSPs of increasing amplitude to determine the relationship between V_{peak} and stimulus strength (Fig. 1d). In all experiments, inhibitory synaptic transmission was blocked using $GABA_A$ and $GABA_B$ receptor antagonists.

Next, we applied the organic antagonist ZD7288 to block I_h and repeated the above measurements of resting membrane properties, voltage sag and EPSP input-output curve. Relatively low concentrations of ZD7288 (10 μM) and short exposure times (10–15 min) were used to minimize nonspecific effects of this drug on synaptic transmission33. These conditions were sufficient to eliminate the voltage sag in response to hyperpolarizing currents, indicating effective block of I_h (Fig. 1c). The average sag ratio decreased from 10.2 ± 1.0% under control conditions to −3.1 ± 0.5% in the presence of ZD7288 ($n=7$, $p < 0.001$, paired t-test). Application of ZD7288 also shifted the resting membrane potential (RMP) by

~ 5 mV to more negative voltages (RMP under control conditions equaled −68.9 ± 1.5 mV; RMP in ZD7288 equaled −74.0 ± 1.4 mV; n=7; $p < 0.001$, paired t-test), and increased the input resistance by > 2-fold (control: 138.6 ± 8.2 MΩ; ZD7288: 287.8 ± 25.1 MΩ, n=7; $p < 0.001$, paired t-test), consistent with previous findings19, 23, 24, 26, 34.

A comparison of EPSP input-output curves in the presence and absence of ZD7288 showed that the effects of I_h on peak EPSP voltage depended on EPSP size (Fig. 2). For small EPSPs, the presence of I_h increased V_{peak}, shifting it to more positive potentials as expected for an inward, excitatory current (Fig. 2a, 30 μA stimulus). However, as the stimulus strength was increased to evoke larger EPSPs, V_{peak} in the absence of I_h approached its value in the presence of I_h (Fig. 2a, 45 μA stimulus). Eventually with even stronger stimuli, a crossover occurred, where the presence of I_h decreased the peak EPSP voltage to values more negative than those reached in the absence of I_h (Fig. 2a, 60 μA stimulus). This depolarizing/hyperpolarizing crossover effect was clearly seen when V_{peak} was plotted as a function of stimulus strength in the presence and absence of I_h (Fig. 2b). Surprisingly, the crossover occurred for subthreshold EPSPs whose peak voltages were well below the I_h reversal potential of −30 mV, that is, at voltages where I_h provided an inward, depolarizing current.

Subthreshold hyperpolarizing effects of I_h on V_{peak} were seen in 6 out of 7 cells that we examined. The one exception occurred in a cell whose resting potential in the presence of I_h was unusually positive (−64 mV) so that spikes were evoked with small current stimuli (35 μA). In some cells, crossover occurred well below the action potential threshold, providing clear evidence that I_h can exert an unambiguously inhibitory influence on subthreshold EPSP peak voltage (see Fig 2b). In other cells, the crossover from depolarizing to hyperpolarizing effects occurred near threshold (Fig. 2c). In such cells V_{peak} in the presence of ZD7288 approached or overlapped with V_{peak} in the absence of drug up to potentials very near spike threshold. A slight increase in stimulus intensity could then evoke spikes in the presence but not absence of ZD7288. Such results are consistent with previous findings that I_h has a paradoxical effect to inhibit spiking17-19, 23.

I_h is purely excitatory when the sole active conductance

How can we explain the inhibitory effect of I_h to reduce the peak EPSP voltage at potentials negative to the I_h reversal potential? As discussed in the Introduction, whereas the depolarizing current carried by I_h should make V_{peak} more positive, the shunting effect of the I_h conductance is expected to decrease V_{peak}. To determine whether these two opposing effects of I_h could yield a net inhibitory influence on V_{peak}, we first examined a single-compartment computational model containing only a passive leak conductance, a physiologically-realistic model of I_h10, 17, and a linear excitatory synaptic conductance modeled as an alpha function35 (Fig. 3a). We determined the V_{peak} attained for different strengths of synaptic input when either the maximal conductance of I_h or the voltage at which I_h was half-maximally activated ($V_{1/2}$) was varied across a range of physiologically and experimentally relevant values10, 17.

When we increased I_h by increasing its maximal conductance, the resting membrane potential was shifted to more positive values as expected. Similarly, depolarizing shifts of

$V_{1/2}$, which increased resting I_h, also depolarized the membrane (Fig. 3b). Enhancing I_h by either method diminished the EPSP amplitude (ΔV_{EPSP}) for all synaptic strengths examined (Fig. 3c). These results confirmed previously reported findings for I_h10, 17, 21.

Despite the effect of I_h to decrease ΔV_{EPSP}, the increase in I_h always had a depolarizing effect on the peak EPSP voltage, as long as the membrane potential was negative to the I_h reversal potential of −30 mV (Fig. 3d,e). I_h did shift V_{peak} to more negative potentials for very large synaptic conductances that drove V_{peak} positive to E_h, where I_h provided an outward current that hyperpolarized the membrane. Thus, because the threshold for firing a spike is negative to −30 mV (typically around −50 mV), our results show that I_h, in the absence of other voltage-gated conductances, was always excitatory for subthreshold EPSPs. This excitatory effect of I_h persisted even when its maximal conductance was varied by 100-fold (Fig. 3e), mimicking the range of I_h conductances reported along the somatodendritic gradient in CA1 and layer V neocortical pyramidal neurons8-11, 36. We also observed an excitatory effect on V_{peak} when the magnitude of I_h was increased by a shift in its voltage-dependence of activation to more positive potentials (Supplementary Fig. 1a).

One well-characterized effect of I_h is to reduce temporal summation during a burst of EPSPs, an effect that has been attributed to the action of the I_h conductance to decrease the membrane time constant and to the hyperpolarization caused by the deactivation of I_h during the burst of EPSPs14-15. Our simulations confirmed that I_h did decrease the extent of temporal summation during a 100 Hz burst of 5 EPSPs. However, even during the burst, the net effect of I_h on membrane voltage was still excitatory, with the peak EPSP voltage during the burst reaching more positive potentials in the presence of I_h than in its absence (Supplementary Figs. 2a, 3a).

Previous studies reported a particularly strong inhibitory effect of I_h when its action to depolarize the resting membrane is compensated by injection of hyperpolarizing current or a reduction in external K^+ concentration17-19, 23, 34. Such results are not surprising because when changes in resting potential are prevented the inhibitory effect of I_h to enhance the membrane conductance should predominate. Indeed, when we simulated this protocol by adjusting the leak conductance reversal potential to keep the resting potential constant, an increase in I_h had a marked inhibitory effect on V_{peak} (Supplementary Fig. 1b). However, the more important question is how does I_h exert its inhibitory effect on V_{peak} when the resting potential is free to adopt its intrinsic value, as occurs under physiological conditions.

I_h interacts with a K^+ current to inhibit EPSPs

Our computational results above demonstrated a purely excitatory effect of I_h on subthreshold EPSPs and thus suggested that the inhibitory effect of I_h on large EPSPs observed in our experiments must involve an interaction with other voltage-gated conductances. One possibility we considered is that the resting membrane depolarization caused by the presence of I_h may increase the activation of a low-threshold voltage-gated K^+ conductance, and that this interaction may have a net inhibitory impact on the peak voltage of the EPSP. To test this, we extended our computational model by adding a Hodgkin-Huxley delayed-rectifier K^+ conductance35, 37 and repeated the above simulations.

In the presence of the delayed rectifier K^+ conductance, an increase in I_h always depolarized the resting membrane and diminished EPSP amplitude (ΔV_{EPSP}), as seen in the single-conductance model (Supplementary Fig. 4a,b). However, inclusion of the voltage-gated K^+ conductance now revealed a clear inhibitory effect of I_h on EPSP peak voltage. For small EPSPs, I_h still exerted a net depolarizing influence on V_{peak} (Fig. 4a, left), as observed in the model with I_h alone. However, for larger EPSPs, I_h now exerted a hyperpolarizing influence on V_{peak} (Fig. 4a,right). This inhibitory effect was observed even when the peak EPSP voltage was negative to both the reversal potential of I_h (−30 mV) and typical values for action potential threshold (−50 mV) (Fig. 4b). Thus, these computational results reproduced the key findings of our synaptic stimulation experiments, including the presence of a subthreshold crossover voltage at which I_h shifted from having a depolarizing effect on V_{peak} to having a hyperpolarizing influence (Fig. 4b). As observed in the model with I_h alone, when the resting potential was held fixed (by altering the leak conductance reversal potential), I_h had a purely inhibitory effect, reducing V_{peak} at all synaptic strengths (Supplementary Fig. 4c).

Which biophysical properties of the voltage-gated K^+ conductance are required to enable the subthreshold inhibitory effects of I_h? We first examined the importance of the K^+ conductance kinetics by making the rate of activation infinitely slow, such that the K^+ conductance remained at its initial equilibrium value set by the resting potential during the entire time course of the EPSP. Under these conditions I_h still exerted a dual depolarizing/hyperpolarizing influence (Fig. 4c), increasing V_{peak} for small EPSPS but reducing V_{peak} for larger subthreshold EPSPs. In contrast, when we made the activation rate infinitely fast, so that the K^+ conductance attained its steady-state level of activation instantaneously throughout the EPSP, I_h now exerted a purely excitatory effect (Fig. 4d), shifting V_{peak} to more depolarized values for all EPSP sizes. Thus, the ability of I_h to inhibit V_{peak} requires that the I_h-dependent enhancement in steady-state resting K^+ conductance persists throughout the EPSP.

Next we examined how shifting the steady-state voltage-dependence of K^+ current activation affects the ability of I_h to influence the EPSP. We found that the crossover voltage at which I_h changes from having a depolarizing influence on V_{peak} to having a hyperpolarizing influence became more negative as the voltage-dependence of K^+ conductance activation was shifted to more hyperpolarized potentials. Conversely, depolarizing shifts in K^+ current activation properties moved the crossover voltage to more positive potentials (data not shown). Importantly, a subthreshold crossover voltage, and hence an inhibitory effect of I_h, was observed over a wide voltage range of K^+ current activation parameters, indicating a robust effect.

I_h interacts with the M-type K^+ current to inhibit EPSPs

Because the above computational results relied on the squid axon K^+ conductance, it was important to explore whether a model incorporating a mammalian voltage-gated K^+ conductance could also interact appropriately with I_h to yield subthreshold inhibitory effects. We reasoned that the K_V7 M-type K^+ current was a good candidate to mediate the inhibitory effects of I_h as the M-current is present in CA1 pyramidal neurons, activates at subthreshold

voltages, exhibits a slow time course of activation, and displays non-inactivating gating properties38-41. We therefore examined a model containing I_h, a passive leak conductance, an excitatory synaptic input, and a model of the M-current based on previously published studies in mammalian pyramidal neurons42, 43.

We found that the M-current also enabled I_h to exert a dual depolarizing/hyperpolarizing effect on the peak voltage of subthreshold EPSPs. As observed with the Hodgkin-Huxley K^+ conductance model, I_h interacted with M-current to depolarize the peak voltage of weak EPSPs but to hyperpolarize V_{peak} for stronger but still subthreshold EPSPs (Fig. 4e). Also similar to the Hodgkin-Huxley K^+ conductance, shifts in the $V_{1/2}$ of M-current activation (Fig. 5a,b) or changes in M-current maximal conductance (Fig. 5c,d) altered the crossover voltage at which I_h began to exert an inhibitory influence. In the presence of M-current, I_h was also able to exert a net inhibitory effect on peak voltage during a burst of strong EPSPs, as observed previously14-15, although the influence of I_h by the final EPSP was minimal due to its deactivation during the burst (Supplementary Figs. 2b,c and 3b,c).

In contrast to the crossover in the EPSP input-output curves in response to changes in I_h, a comparison of EPSP input-output curves with or without M-current revealed that this K^+ current exerted a purely inhibitory effect, shifting peak EPSP voltage to more negative potentials at all synaptic strengths. This inhibitory action of M-current was seen either in the absence or presence of a fixed level of I_h (data not shown). Such an effect is consistent with previous results that the M-current inhibits neural activity40-41.

So far we have considered the interaction of I_h and M-current in the context of a single compartment model. However, I_h is present in a gradient of increasing density along the apical dendritic tree of both CA1 and layer 5 pyramidal neurons, where I_h density at the distal tips of the dendrites is up to 50-fold larger than that in the soma8, 9, 11. In contrast, the precise subcellular localization of the M-type K^+ channels is less clear, with some studies reporting dendritic M-currents38, 41 versus others claiming only somatic and/or axonal localization40, 44. To examine the importance of the subcellular localization of these channels, we incorporated the I_h dendritic gradient into a multicompartment model of a CA1 neuron in which excitatory inputs were targeted to the apical dendrites. Importantly, an inhibitory effect of I_h on the somatic peak EPSP voltage was still observed, regardless of whether M-current was present in dendrites or restricted to the soma (Supplementary Fig. 5b,c). When M-current was restricted to the soma, dendritic I_h exerted a purely depolarizing effect on the local dendritic EPSPs recorded at the site of synaptic input, 250 μm from the soma. However, the dendritic I_h still was able to inhibit the peak somatic voltage for large, subthreshold EPSPs. Conversely, in multicompartment models lacking an M-current, I_h produced a purely depolarizing effect on both local dendritic EPSPs and somatic EPSPs (Supplementary Fig. 5a). These results clearly show that the inhibitory effects of I_h on somatic EPSPs require the presence of M-type K^+ channels but are not very sensitive to the subcellular distribution of either I_h or M-current.

Inhibitory effects of I_h prevented by M-current blockade

We next took an experimental approach to examine whether the inhibitory effects of I_h in CA1 neurons do indeed arise from its interaction with the M-current by applying the specific

M-current inhibitor XE99130, 39, 40, using a drug concentration (10 μM) that does not alter synaptic transmission under the conditions of our experiments44. Application of XE991 produced a variable depolarization of the resting membrane that was large enough to lead to spontaneous firing in some CA1 neurons, consistent with the inhibitory role of the M-current. Such cells were not studied further because the spiking interfered with EPSP measurements. In those cells that did not fire spontaneously, XE991 produced a relatively small 3.4 mV ($p = 0.10$; n=7) depolarization of the resting membrane (Fig. 6d).

Next we examined the effects of I_h on somatic EPSPs with M-current blocked by measuring V_{peak} as a function of stimulus strength, first in the presence of I_h and then following I_h blockade with ZD7288. Addition of ZD7288 in the presence of XE991 hyperpolarized the resting membrane by ∼ 8 mV (RMP in XE991 alone = −65.5 ± 1.7 mV; RMP in XE991 + ZD7288 = −73.5 ± 1.8 mV; n = 7, $p < 0.001$, paired t-test), similar to its effect in the absence of XE991. Of particular interest, blockade of the M-current abolished the inhibitory effect of I_h, which now exerted a purely excitatory effect on the peak EPSP voltage for both weak and strong stimuli (Fig 6a-c; compare to Fig. 2 with normal M-current). This result was seen in all cells tested (n=7). In addition, when M-current was blocked, the presence of I_h now increased the excitability of the cell, as evidenced by spike firing at lower stimulus strengths in the absence of ZD7288 than in its presence (Fig 6a, right panel). These findings confirm the modeling results and further support the idea that I_h alone exerts an excitatory influence on neuronal activity and that the inhibitory effects of I_h require an interaction with voltage-gated K^+ currents.

DISCUSSION

Here we found that I_h exerts dual depolarizing/hyperpolarizing effects on the peak voltage of subthreshold EPSPs as a function of synaptic strength. For weak EPSPs, I_h exerts a depolarizing effect on V_{peak}. In contrast, for strong EPSPs, I_h exerts an inhibitory, hyperpolarizing effect. Whereas previous studies described an inhibitory influence of I_h on EPSP amplitude (ΔV_{EPSP}) and firing of both Na^+ and Ca^{2+} spikes10, 15, 17, 19, 23, 26, our results provide the first demonstration that I_h can also exert an inhibitory effect on subthreshold peak EPSP voltage. This is an important distinction because peak EPSP voltage, rather than EPSP amplitude, determines the impact of the EPSP on neuronal firing25.

Our results also provide insight into the mechanism of the paradoxical effect by which the depolarizing inward I_h can produce a net hyperpolarizing effect on peak EPSP voltage. First, using a simple computational model, we found that I_h acting in the absence of other voltage-gated channels exerts a purely depolarizing effect on the peak membrane potential achieved by subthreshold EPSPs. This indicates that the direct excitatory effect of I_h to depolarize the membrane predominates over its inhibitory effect to increase resting membrane conductance. This direct excitatory effect of I_h also underlies its classical contribution to the pacemaker depolarization that generates rhythmic firing in both cardiac myocytes and certain CNS neurons, such as thalamic relay neurons12, 13.

In contrast to the results of the simple model in which I_h is purely excitatory, we found that I_h produced an inhibitory effect on V_{peak} of large, subthreshold EPSPs in models containing delayed-rectifier voltage-gated K^+ channels. The excitatory to inhibitory crossover effect of I_h on peak EPSP voltage that occurred in such models provides an interesting example of the nonlinear interplay of voltage-dependent currents. The depolarization of the resting membrane by I_h enhances the resting voltage-gated K^+ conductance beyond that attained in the absence of I_h. At the peak of a weak EPSP, the outward driving force on K^+ is quite small compared to the large inward driving force on current through I_h channels, causing the direct depolarizing effect of I_h to be dominant. In contrast, at the peak of large EPSPs, the outward driving force on K^+ is increased and the inward driving force on I_h is decreased. As a result, the inhibitory effect of the K^+ current is dominant. Our computational results further suggest that the inhibitory effect of I_h requires that the K^+ current kinetics be relatively slow compared to the time course of the EPSP. Under these conditions, the inhibitory effect of I_h to enhance the resting K^+ conductance can persist throughout the EPSP.

Both our experimental and computational findings implicate the M-type K^+ current as the likely mediator of the inhibitory effects of I_h in CA1 pyramidal neurons. The relatively negative voltage range of activation of the M-current allows it to respond to the small changes in resting potential mediated by I_h; the slow activation kinetics of the M-current ensure that such changes in resting activation influence the peak EPSP voltage30, 38, 40, 41. Moreover, in experiments where we blocked the M-current with XE991, I_h exerted a purely excitatory effect, confirming that M-current is necessary for the inhibitory effect of I_h. One other important computational result is that the inhibitory effect on somatic peak EPSP voltage caused by the interaction of I_h and M-current does not depend on channel distributions within the somatodendritic compartments. This is important as I_h is known to be present in a gradient of increasing density in apical dendrites whereas it is unclear whether M-current is restricted to axo-somatic compartments or is also present in dendrites38, 40, 41.

In contrast to the dual depolarizing/hyperpolarizing effects of I_h on V_{peak}, all manipulations that increased the M-current, whether in the absence or presence of I_h, hyperpolarized V_{peak}, with no crossover effect. This is consistent with a large number of previous studies showing an inhibitory influence of the M-current40, 41. The purely inhibitory nature of the M-current arises because its two actions to enhance membrane conductance and to generate a hyperpolarizing outward current both act in the same direction to inhibit peak EPSP voltage and neuronal firing. This is in contrast to I_h, whose direct depolarizing and shunting effects have opposing influences.

Interestingly, both I_h and M-current can be modulated by neurotransmitters and second messenger cascades, raising the possibility that the mode of action of I_h on dendritic integration can be tuned from inhibition to excitation. For example, both cyclic nucleotides45 and phosphatidylinositol (4,5)-bisphosphate (PIP_2)46, 47 shift the voltage dependence of I_h activation to more positive potentials. As we reported above, upregulating I_h has a depolarizing effect on small EPSPs but an inhibitory effect on large EPSPs; downregulation of I_h leads to the opposite outcomes. Similarly, a loss of M-current, as

occurs with muscarinic receptor stimulation48 and PIP_2 depletion49, will drive I_h into a purely excitatory mode of action on V_{peak}. In contrast, a large increase in M-current, as occurs in response to an increase in cAMP32, will cause I_h to exert a predominantly inhibitory effect on V_{peak} (see Fig. 5). Changes in both the M-current and I_h have been implicated in epileptic diseases24, 29, 31, 32, and understanding how these two currents interact to regulate excitability may ultimately be important for developing new therapeutic approaches.

The dual depolarizing/hyperpolarizing effects of I_h on peak EPSP voltage have interesting implications for how this current may differentially regulate neuronal firing depending on the state of excitability of a neuron. Under conditions where spike threshold is low and negative to the I_h crossover voltage for inhibition, manipulations that enhance I_h will increase V_{peak} and, thus, have an excitatory effect on the ability of an EPSP to trigger an action potential. In contrast, when spike threshold is high and positive to the crossover voltage, manipulations that enhance I_h will decrease V_{peak} and, thus, inhibit the ability of an EPSP to elicit an output. Thus, the polarity of the effect that a change in I_h exerts on neuronal firing will depend on the overall excitability of the cell. Even if I_h and I_m remain constant, the effect of their interaction on neuronal output can shift from excitatory to inhibitory as a result of modulatory changes in other voltage-gated conductances that alter spike threshold. Such nonlinear subthreshold interactions among voltage-gated channels provide a rich variety of mechanisms to fine-tune the relationship between excitatory synaptic input and neuronal output.

METHODS

Slice Electrophysiology

Whole-cell recordings were obtained from hippocampal CA1 pyramidal cells in submerged horizontal brain slices from P28–P40 mice. Recordings were performed at 31°C–33°C with inhibitory transmission blocked by $GABA_A$ (2 μM gabazine) and $GABA_B$ receptor antagonists (1 μM CGP-55845). Stimulating current pulses (0.1–0.2 ms) were applied through focal extracellular electrodes with a constant current generator once every 15 s. For graded stimulation, current amplitude was adjusted to evoke an EPSP in control conditions and then incremented until spike threshold was reached. Identical current pulses were reapplied after addition of 10 μM ZD7288 to block I_h. All procedures conformed to US National Institutes of Health regulations and were approved by the Institutional Animal Care and Use Committees of Columbia University and the New York State Psychiatric Institute. See Supplementary Information for full details.

Statistical Analysis

Average sag ratio expressed as $[(1 - \Delta V_{ss} / \Delta V_{min}) \times 100\%]$ where $\Delta V_{ss} = RMP - V_{ss}$ and $\Delta V_{min} = RMP - V_{min}$. Comparisons were made using paired t-tests where appropriate. An unpaired t-test was used to compare control RMP to XE RMP. p values less than 0.05 were considered statistically significant. Results expressed as mean ± S.E.

Computational Modeling

Computational models were implemented and run in NEURON50 (version 5.9; http://www.neuron.yale.edu/neuron). The I_h10, 17 and M-type K^+ conductance40,42, 43 models were based on experimental studies. See Supplementary Information for full details.

Supplementary Material

Refer to Web version on PubMed Central for supplementary material.

ACKNOWLEDGEMENTS

We thank Joshua Dudman for helpful advice and for providing custom data acquisition routines written in Igor. This work was partially supported by grant MH80745 from NIH to S.A.S. L.A and M.S.G. supported in part by an NIH Director's Pioneer Award, part of the NIH Roadmap for Medical Research, through grant number 5-DP1-OD114-02. M.S.G. was supported in part by Columbia University's Medical Scientist Training Program.

REFERENCES

1. Migliore M, Shepherd GM. Emerging rules for the distributions of active dendritic conductances. Nat Rev Neurosci. 2002:362–370. [PubMed: 11988775]
2. Magee JC, Johnston D. Synaptic activation of voltage-gated channels in the dendrites of hippocampal pyramidal neurons. Science. 1995:301–304. [PubMed: 7716525]
3. Golding NL, Staff NP, Spruston N. Dendritic spikes as a mechanism for cooperative long-term potentiation. Nature. 2002:326–331. [PubMed: 12124625]
4. Losonczy A, Magee JC. Integrative properties of radial oblique dendrites in hippocampal CA1 pyramidal neurons. Neuron. 2006:291–307. [PubMed: 16630839]
5. Frick A, Magee J, Johnston D. LTP is accompanied by an enhanced local excitability of pyramidal neuron dendrites. Nat Neurosci. 2004:126–135. [PubMed: 14730307]
6. Losonczy A, Makara JK, Magee JC. Compartmentalized dendritic plasticity and input feature storage in neurons. Nature. 2008:436–441. [PubMed: 18368112]
7. Ngo-Anh TJ, et al. SK channels and NMDA receptors form a Ca2+-mediated feedback loop in dendritic spines. Nat Neurosci. 2005:642–649. [PubMed: 15852011]
8. Kole MH, Hallermann S, Stuart GJ. Single Ih channels in pyramidal neuron dendrites: properties, distribution, and impact on action potential output. J Neurosci. 2006:1677–1687. [PubMed: 16467515]
9. Lorincz A, Notomi T, Tamas G, Shigemoto R, Nusser Z. Polarized and compartment-dependent distribution of HCN1 in pyramidal cell dendrites. Nat Neurosci. 2002:1185–1193. [PubMed: 12389030]
10. Magee JC. Dendritic hyperpolarization-activated currents modify the integrative properties of hippocampal CA1 pyramidal neurons. J Neurosci. 1998:7613–7624. [PubMed: 9742133]
11. Notomi T, Shigemoto R. Immunohistochemical localization of Ih channel subunits, HCN1-4, in the rat brain. J Comp Neurol. 2004:241–276. [PubMed: 14991560]
12. Luthi A, McCormick DA. H-current: properties of a neuronal and network pacemaker. Neuron. 1998:9–12. [PubMed: 9697847]
13. Robinson RB, Siegelbaum SA. Hyperpolarization-activated cation currents: from molecules to physiological function. Annu Rev Physiol. 2003:453–480. [PubMed: 12471170]
14. Angelo K, London M, Christensen SR, Häusser M. Local and global effects of I(h) distribution in dendrites of mammalian neurons. J Neurosci. 2007:8643–8653. [PubMed: 17687042]
15. Magee JC. Dendritic lh normalizes temporal summation in hippocampal CA1 neurons. Nat Neurosci. 1999:508–514. [PubMed: 10448214]
16. Williams SR, Stuart GJ. Site independence of EPSP time course is mediated by dendritic I(h) in neocortical pyramidal neurons. J Neurophysiol. 2000:3177–3182. [PubMed: 10805715]

17. Poolos NP, Migliore M, Johnston D. Pharmacological upregulation of h-channels reduces the excitability of pyramidal neuron dendrites. Nat Neurosci. 2002:767–774. [PubMed: 12118259]
18. Rosenkranz JA, Johnston D. Dopaminergic regulation of neuronal excitability through modulation of Ih in layer V entorhinal cortex. J Neurosci. 2006:3229–3244. [PubMed: 16554474]
19. Fan Y, et al. Activity-dependent decrease of excitability in rat hippocampal neurons through increases in I(h). Nat Neurosci. 2005:1542–1551. [PubMed: 16234810]
20. Narayanan R, Johnston D. Long-term potentiation in rat hippocampal neurons is accompanied by spatially widespread changes in intrinsic oscillatory dynamics and excitability. Neuron. 2007:1061–1075. [PubMed: 18093527]
21. Nolan MF, et al. A behavioral role for dendritic integration: HCN1 channels constrain spatial memory and plasticity at inputs to distal dendrites of CA1 pyramidal neurons. Cell. 2004:719–732. [PubMed: 15550252]
22. Stuart G, Spruston N. Determinants of voltage attenuation in neocortical pyramidal neuron dendrites. J Neurosci. 1998:3501–3510. [PubMed: 9570781]
23. Brager DH, Johnston D. Plasticity of intrinsic excitability during long-term depression is mediated through mGluR-dependent changes in I(h) in hippocampal CA1 pyramidal neurons. J Neurosci. 2007:13926–13937. [PubMed: 18094230]
24. Shah MM, Anderson AE, Leung V, Lin X, Johnston D. Seizure-induced plasticity of h channels in entorhinal cortical layer III pyramidal neurons. Neuron. 2004:495–508. [PubMed: 15504329]
25. Koch C, Bernander O, Douglas RJ. Do neurons have a voltage or a current threshold for action potential initiation? Journal of computational neuroscience. 1995:63–82. [PubMed: 8521281]
26. Tsay D, Dudman JT, Siegelbaum SA. HCN1 channels constrain synaptically evoked Ca2+ spikes in distal dendrites of CA1 pyramidal neurons. Neuron. 2007:1076–1089. [PubMed: 18093528]
27. Delmas P, Brown DA. Pathways modulating neural KCNQ/M (Kv7) potassium channels. Nat Rev Neurosci. 2005:850–862. [PubMed: 16261179]
28. Wang M, et al. Alpha2A-adrenoceptors strengthen working memory networks by inhibiting cAMP-HCN channel signaling in prefrontal cortex. Cell. 2007:397–410. [PubMed: 17448997]
29. Chen K, et al. Persistently modified h-channels after complex febrile seizures convert the seizure-induced enhancement of inhibition to hyperexcitability. Nat Med. 2001:331–337. [PubMed: 11231632]
30. Jentsch TJ. Neuronal KCNQ potassium channels: physiology and role in disease. Nat Rev Neurosci. 2000:21–30. [PubMed: 11252765]
31. Peters HC, Hu H, Pongs O, Storm JF, Isbrandt D. Conditional transgenic suppression of M channels in mouse brain reveals functions in neuronal excitability, resonance and behavior. Nat Neurosci. 2005:51–60. [PubMed: 15608631]
32. Schroeder BC, Kubisch C, Stein V, Jentsch TJ. Moderate loss of function of cyclic-AMP-modulated KCNQ2/KCNQ3 K+ channels causes epilepsy. Nature. 1998:687–690. [PubMed: 9872318]
33. Chevaleyre V, Castillo PE. Assessing the role of Ih channels in synaptic transmission and mossy fiber LTP. Proc Natl Acad Sci U S A. 2002:9538–9543. [PubMed: 12093909]
34. Gu N, Vervaeke K, Hu H, Storm JF. Kv7/KCNQ/M and HCN/h, but not KCa2/SK channels, contribute to the somatic medium after-hyperpolarization and excitability control in CA1 hippocampal pyramidal cells. J Physiol. 2005:689–715. [PubMed: 15890705]
35. Dayan, Peter; Abbott, LF. Theoretical Neuroscience: Computational and Mathematical Modeling of Neural Systems. 2005:576.
36. Santoro B, et al. Molecular and functional heterogeneity of hyperpolarization-activated pacemaker channels in the mouse CNS. J Neurosci. 2000:5264–5275. [PubMed: 10884310]
37. Hodgkin AL, Huxley AF. A quantitative description of membrane current and its application to conduction and excitation in nerve. The Journal of Physiology. 1952:500–544. [PubMed: 12991237]
38. Chen X, Johnston D. Properties of single voltage-dependent K+ channels in dendrites of CA1 pyramidal neurones of rat hippocampus. J Physiol. 2004:187–203. [PubMed: 15218076]

39. Hu H, Vervaeke K, Storm JF. Two forms of electrical resonance at theta frequencies, generated by M-current, h-current and persistent Na+ current in rat hippocampal pyramidal cells. J Physiol. 2002:783–805. [PubMed: 12482886]
40. Hu H, Vervaeke K, Storm JF. M-channels (Kv7/KCNQ channels) that regulate synaptic integration, excitability, and spike pattern of CA1 pyramidal cells are located in the perisomatic region. J Neurosci. 2007:1853–1867. [PubMed: 17314282]
41. Yue C, Yaari Y. Axo-somatic and apical dendritic Kv7/M channels differentially regulate the intrinsic excitability of adult rat CA1 pyramidal cells. J Neurophysiol. 2006:3480–3495. [PubMed: 16495357]
42. Kole MH, et al. Action potential generation requires a high sodium channel density in the axon initial segment. Nat Neurosci. 2008:178–186. [PubMed: 18204443]
43. Poirazi P, Brannon T, Mel BW. Arithmetic of subthreshold synaptic summation in a model CA1 pyramidal cell. Neuron. 2003:977–987. [PubMed: 12670426]
44. Vervaeke K, Gu N, Agdestein C, Hu H, Storm JF. Kv7/KCNQ/M-channels in rat glutamatergic hippocampal axons and their role in regulation of excitability and transmitter release. J Physiol. 2006:235–256. [PubMed: 16840518]
45. Wainger BJ, DeGennaro M, Santoro B, Siegelbaum SA, Tibbs GR. Molecular mechanism of cAMP modulation of HCN pacemaker channels. Nature. 2001:805–810. [PubMed: 11459060]
46. Pian P, Bucchi A, Decostanzo A, Robinson RB, Siegelbaum SA. Modulation of cyclic nucleotide-regulated HCN channels by PIP(2) and receptors coupled to phospholipase C. Pflugers Arch. 2007:125–145. [PubMed: 17605039]
47. Zolles G, et al. Pacemaking by HCN channels requires interaction with phosphoinositides. Neuron. 2006:1027–1036. [PubMed: 17178405]
48. Brown DA, Adams PR. Muscarinic suppression of a novel voltage-sensitive K+ current in a vertebrate neurone. Nature. 1980:673–676. [PubMed: 6965523]
49. Suh BC, Inoue T, Meyer T, Hille B. Rapid chemically induced changes of PtdIns(4,5)P2 gate KCNQ ion channels. Science. 2006; 314:1454–1457. [PubMed: 16990515]
50. Carnevale NT, Hines ML. The NEURON book. 2006

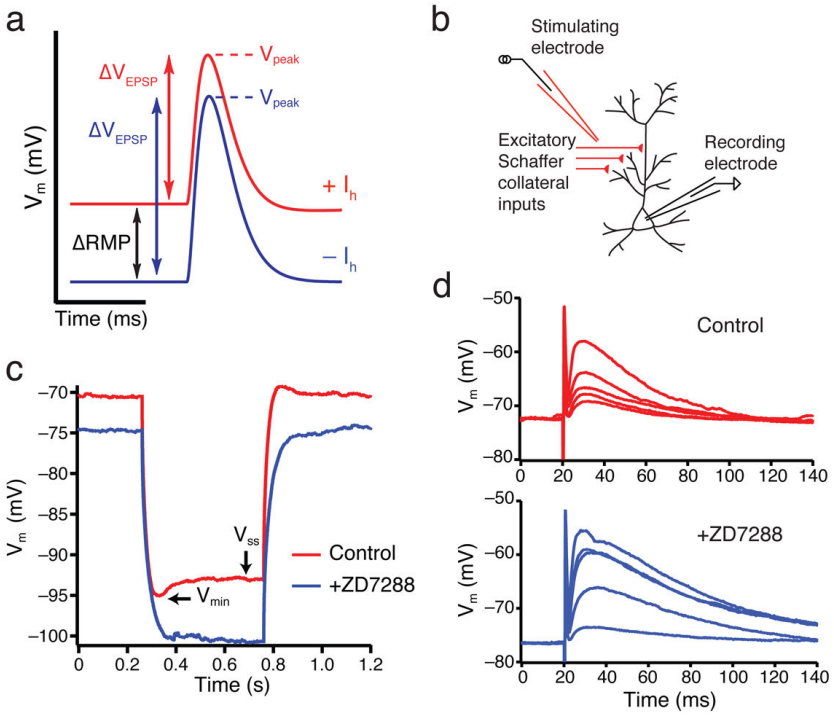

Figure 1. Experimental paradigm and effects of pharmacological blockade of I_h

(a) Diagram illustrating the opposing effects of I_h on subthreshold EPSPs, involving a positive shift of the resting membrane potential (RMP) and a decrease in the EPSP amplitude (ΔV_{EPSP}). Red, In presence of I_h; Blue, In absence of I_h. V_{peak}, potential at the peak of the EPSP. $\Delta V_{EPSP} = V_{peak} - RMP$.

(b) Schematic of experimental setup. Whole-cell current-clamp recordings were obtained from CA1 pyramidal neurons (recording patch electrode). An extracellular stimulating patch electrode was placed ∼ 150 μm away from the soma in stratum radiatum under visual guidance. (c) Somatic voltage response to a hyperpolarizing current step in absence (control) and presence of ZD7288 (10 μM). Note the RMP hyperpolarization after application of ZD7288. Under control conditions, the membrane voltage reached an initial minimum value (V_{min}) and then showed a depolarizing sag to a steady-state value (V_{ss}) due to activation of I_h. Hyperpolarizing sag was eliminated by ZD7288. (d) Sample EPSPs evoked in response to a range of stimulus strengths under control conditions and after block of I_h using ZD7288.

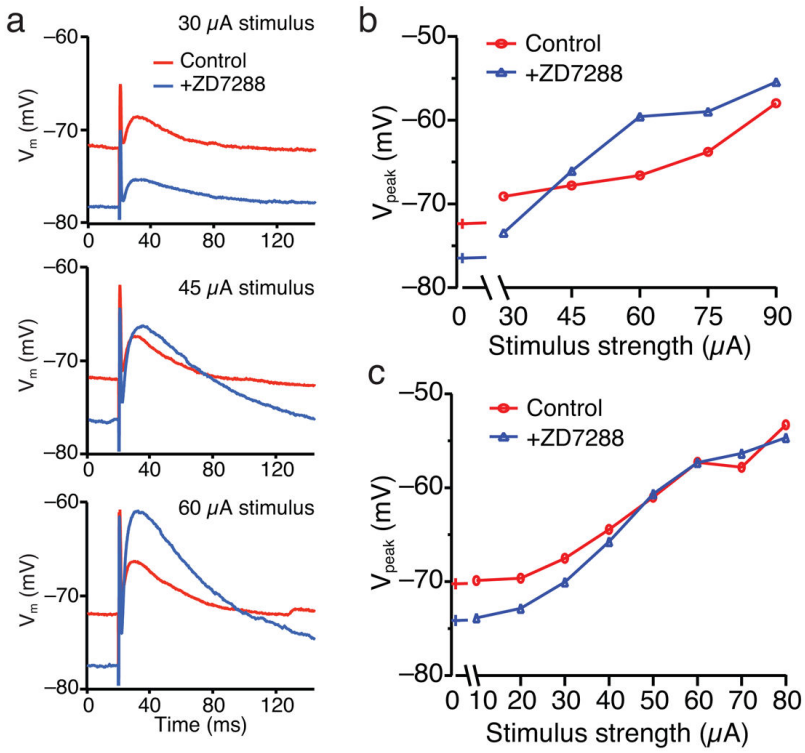

Figure 2. Dual effects of I_h on peak voltage of subthreshold EPSPs

(a) Representative EPSP responses for three stimulus strengths recorded at the soma under control conditions (red) and in the presence of ZD7288 (10 μM) (blue). Top panel: I_h had a depolarizing effect on V_{peak} for a small EPSP elicited by a weak stimulus. Middle panel: For an intermediate strength stimulus, V_{peak} was similar in the presence or absence of I_h. Bottom panel: With a stronger stimulus, I_h had an inhibitory effect so that its blockade led to a more depolarized V_{peak}. (b) Relation between V_{peak} and stimulus current strength in the presence (control, red) or absence (+ZD7288, blue) of I_h. All EPSPs were subthreshold. The 0 μA points (dashes) denote the resting potential. Note that I_h had an inhibitory effect on V_{peak} over a large range of subthreshold stimulus strengths. (c) V_{peak} versus stimulus strength plots for a cell in which I_h had a depolarizing effect on V_{peak} for a large range of weak stimuli. An inhibitory effect of I_h was only observed for a strong stimulus that was just subthreshold.

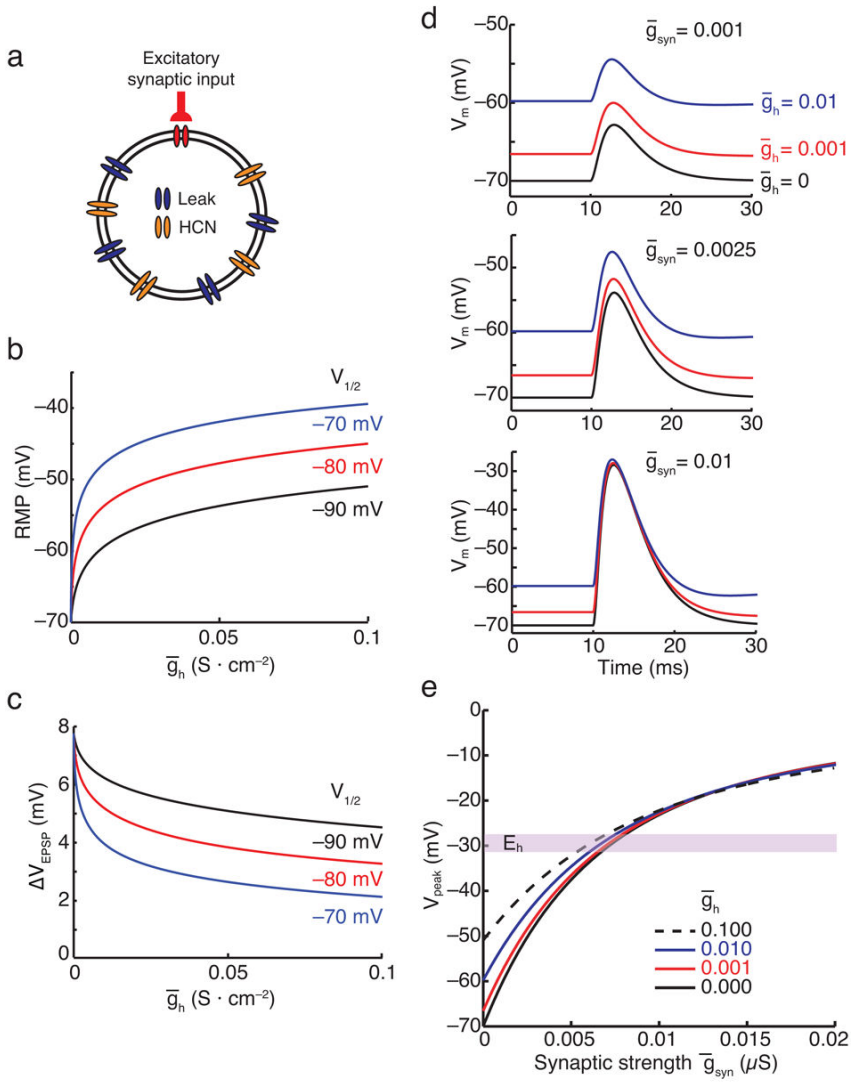

Figure 3. Computational model predicts excitatory role for I_h in absence of other voltage-gated channels

(a) Diagram of the single compartment model containing I_h (HCN channels), a linear leak conductance, and a synaptic conductance (alpha function). (b) Effect of I_h on resting membrane potential (RMP). Increasing maximal I_h conductance ($\bar{g}_h$) or depolarizing shifts of the I_h $V_{1/2}$ produced positive shifts in RMP. (c) Effects of I_h on EPSP amplitude, defined as difference between peak EPSP voltage (V_{peak}) and RMP. Increasing $\bar{g}_h$ or depolarizing shifts of $V_{1/2}$ caused a reduction in EPSP amplitude. Synaptic strength was set to produce an ~ 8 mV EPSP in the absence of I_h. (d) Sample EPSPs from model for various synaptic input strengths ($\bar{g}_{syn}$ in μS) in absence of I_h (black traces) and presence of I_h for two levels of $\bar{g}_h$ (in units of S · cm^{-2}). (e) The effect of I_h on the relation between V_{peak} and synaptic strength ($V_{1/2}$ = −90 mV in d and e). Increasing $\bar{g}_h$ to indicated values had a depolarizing effect on V_{peak} for all membrane potentials below E_h (−30 mV). The y-intercept shows the effect of I_h on RMP.

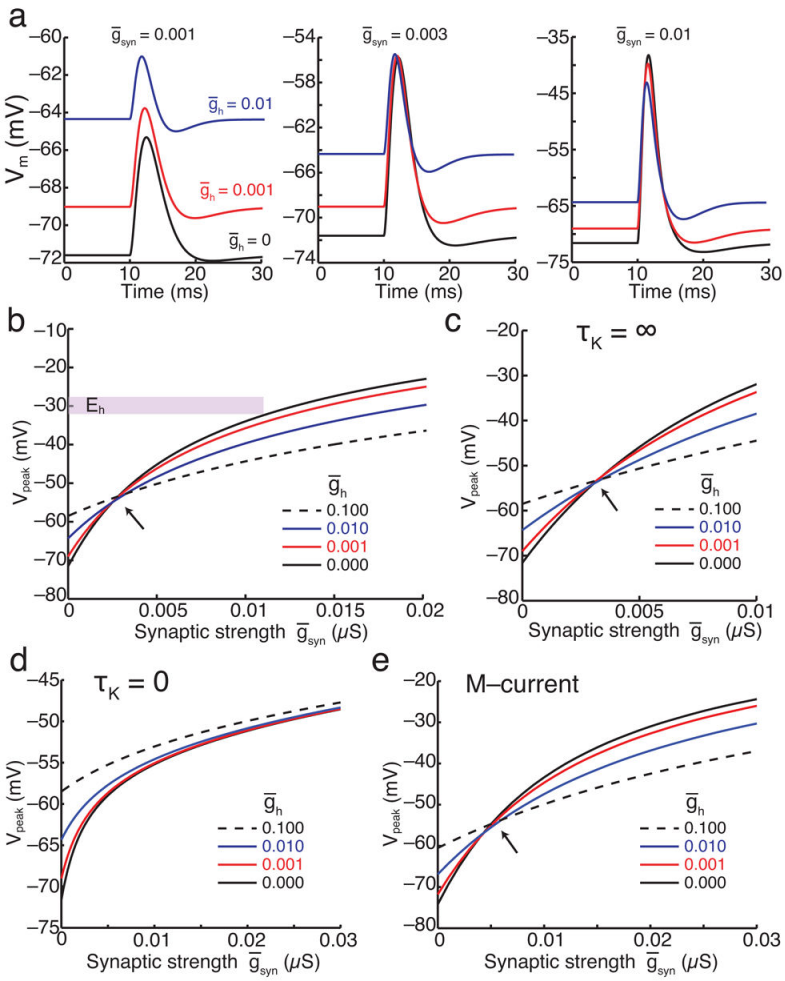

Figure 4. Computational model including a Hodgkin-Huxley voltage-gated K^+ conductance predicts subthreshold inhibitory effects of I_h on peak voltage of strong EPSPs

(a) EPSPs from model for three synaptic input strengths ($\bar{g}_{syn}$) in absence or presence of I_h, for two levels of $\bar{g}_h$ as indicated (I_h: $V_{1/2}$ = −90 mV; I_K: $\bar{g}_{Kdr}$ = 0.036 S · cm^{-2}, $V_{1/2}$ = −52 mV). (b) Effect of I_h on relation between V_{peak} and synaptic strength ($V_{1/2}$ = −90 mV). Increases in $\bar{g}_h$ had a depolarizing effect on V_{peak} for weak synaptic inputs and an inhibitory effect on strong inputs. Notably, the inhibitory regime occurred negative to the I_h reversal potential, E_h (−30 mV). Arrow indicates crossover voltage where I_h changes from a depolarizing to hyperpolarizing influence. (c) Effects of I_h on V_{peak} when the kinetics of delayed-rectifier K^+ conductance activation were made infinitely slow. (d) Effects of I_h on V_{peak} when the kinetics of delayed-rectifier K^+ conductance activation were made infinitely fast. (e) Effects of I_h on V_{peak} in a model containing the mammalian M-type K^+ current ($V_{1/2}$ = −35 mV). Increasing $\bar{g}_h$ in this model also produced mixed depolarizing and hyperpolarizing effects on V_{peak}, with a defined crossover voltage (arrow).

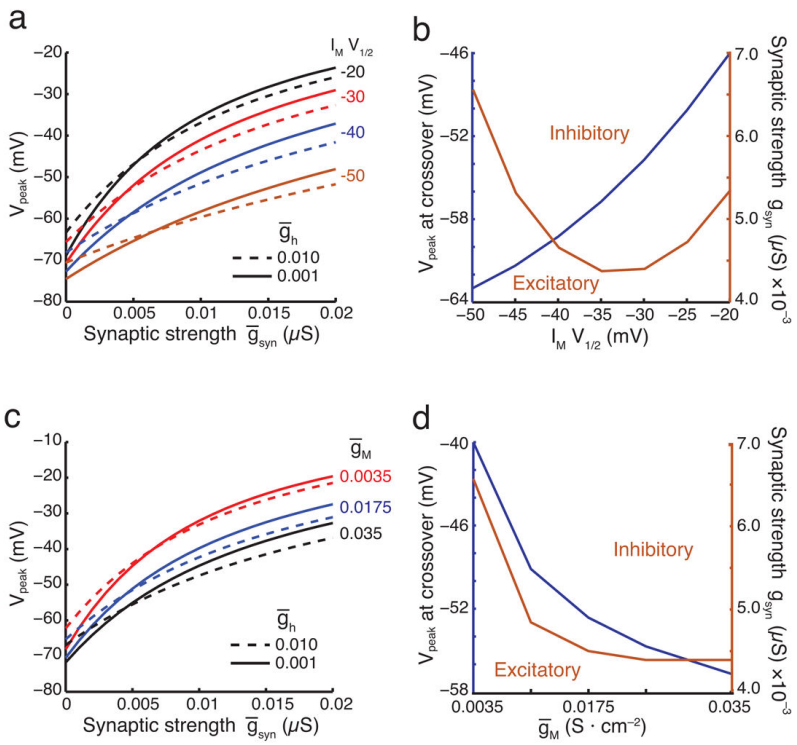

Figure 5. Computational results demonstrating that changes in M-current properties alters crossover voltage at which I_h first exerts an inhibitory influence on EPSP V_{peak}

(a) Effect of I_h on relation between V_{peak} and synaptic strength depends on M-current $V_{1/2}$ values (in mV) ($\bar{g}_M$ equals 0.035 S · cm^{-2} throughout). Crossover voltage in response to an increase in $\bar{g}_h$ was shifted to more negative values as M-current $V_{1/2}$ was made more negative. (b) The effects of M-current $V_{1/2}$ on synaptic conductance magnitude (orange line, right scale) or V_{peak} (blue line, left scale) at which crossover occurred (from data in panel *a*). Regions above the blue or orange lines correspond to V_{peak} or synaptic strength values at which I_h was inhibitory; regions below the line correspond to V_{peak} or synaptic strengths for which I_h depolarized V_{peak}. (c) Effect of I_h on relation between V_{peak} and synaptic strength depends on M-current maximal conductance values ($\bar{g}_M$, S · cm^{-2}) (M-current $V_{1/2}$ = −35 mV). Crossover voltage in response to an increase in $\bar{g}_h$ was shifted to more negative potentials as $\bar{g}_M$ was increased. (d) The effects of varying the maximal M-conductance on V_{peak} (blue line) or synaptic conductance (orange line) at which crossover occurred.

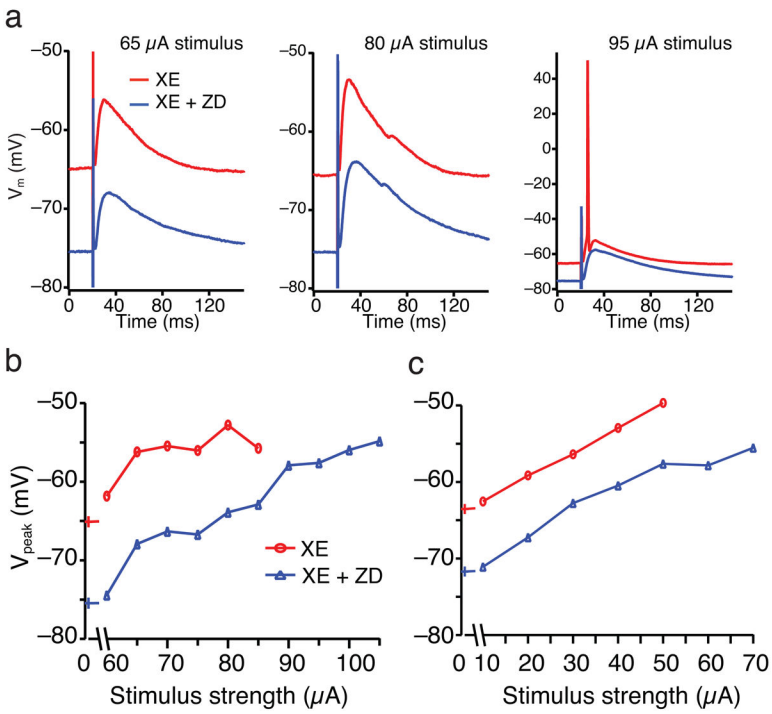

Figure 6. Pharmacological blockade of M-current caused I_h to have a purely excitatory influence

(a) Experimental EPSPs recorded at the soma in response to three stimulus strengths when M-current was blocked with XE991 (10 μM). EPSPs shown in XE991 (XE, red traces) and XE991 plus 10 μM ZD7288 (XE + ZD, blue traces). Presence of I_h had an excitatory effect on V_{peak} for weak (left panel), intermediate (middle panel) and strong (right panel) stimuli. Note strongest stimulus evoked a spike in the presence of I_h but not in its absence. (b) I_h had an excitatory effect on relation between V_{peak} and stimulus strength with M-current blocked by XE991. Data shown in the absence (red) or presence (blue) of ZD7288. The 0 μA data (dashes) denote the RMP. (c) Similar results as in (b) for a second cell.